

Widely Tunable MEMS LC Tank for Multi-Band Applications

A. CAZZORLA¹, P. FARINELLI¹, F. GIACOMOZZI², R. SORRENTINO³

¹RF Microtech, via Mascagni 11, 06132 Perugia, Italy

²Fondazione Bruno Kessler FBK, Via Sommarive 18, I-38123 Povo Trento, Italy

³University of Perugia, Perugia, Italy

Abstract. This paper presents the modeling and simulations of compact multi-band MEMS based LC tank resonator suitable for very low phase-noise VCO. The resonator is based on a high-Q spiral inductor and high capacitive ratio varicap fully integrated in FBK-irst MEMS manufacturing process. The design of the varicap is based on double actuation mechanism with a mechanical central bond that inhibits the pull-in allowing for a theoretically infinite tuning ratio. The measurements show a total *Capacitance ratio* (Cr) of 5.2 with two continuous tuning range with a $Cr^* = 1.6$ and 2.6. The spiral inductor consists of a suspended gold membrane thick 5 μ m in circular shape. The simulations show that the MEMS based resonator allows for an overall tuning range of 60% in the frequency range 2.15 - 3.85GHz. Two separate regions of continuous tuning range (9.5% and 30%) allow one to cover the whole frequency spectrum of WiMAX and IEEE802.11a/b/g/n. The simulated quality factor (Q) is about 60. A preliminary design of the MEMS based *Voltage Controlled Oscillator* (VCO) was performed using *Advanced Design System* (ADS®). Bonding wire interconnections have been also considered and optimized for improved performance. The VCO prototype is being fabricated on *Surface Mount Technology* (SMT) on RO4350 laminate.

Key words: MEMS; Quality Factor; Spiral Inductor; VCO; Varactor;

1. Introduction

With the recent developments in the wireless communication industry, the demands for radios covering the whole frequency spectrum of fixed and mobile WiMAX, and IEEE 802.11a/b/g/n is desired together with minimum hardware resources and costs [1, 2]. In many RF transceiver systems, the voltage controlled oscillators (VCO) are key components since they are the source of the reference oscillation frequency. In conventional harmonic VCO, oscillation frequency is basically determined by the resonant circuit (typically an LC circuit called LC

tank) and the frequency tuning can be achieved by varying the voltage dependent capacitance of the varicap element in the LC tank. Low phase noise and wide tuning range are the main requirements, imposed by the market, for the design of a VCO to be used in new generation front-end circuits.

As reported in literature [3], the phase noise of a VCO depends on many factors like oscillator output power, output oscillation frequency, operating temperature and quality factor (Q) of the LC resonant circuit. The latter is considerably limited by the losses of the passive elements, such as on-chip spiral inductors [4], as well as substrate and conductor losses. In addition, the use of on-chip spiral inductors is limited in frequency by their *self-resonance frequency* (SRF). At this frequency, the coupling capacitance between inductor eddy current and the substrate forms a parallel resonance [5]. It represents a limiting factor if high inductance values are required. In conventional CMOS fabrication process, much effort has been devoted to the enhancement of inductor performance in terms of Q-factor and self-resonance frequency, as reported in [6, 7]. An alternative to conventional CMOS fabrication process is represented by the micro-electromechanical (MEMS) technology [8] which allows to achieve highly miniaturized LC resonators with high-Q performance.

This paper presents a compact multi-band MEMS LC series resonator based on a spiral inductor and a varicap, fully integrated in MEMS manufacturing process. The MEMS based LC tank allows one to design a VCO that can simultaneously operate in the IEEE 802.11b/g (WLAN) and IEEE 802.16d (WiMAX) standards. Measurement results of the MEMS varicap together with mechanical and electromagnetic analyses of high-Q MEMS spiral inductor are presented. Finally, the modeling of the MEMS based LC tank, accounting for bonding wires interconnection, is shown and the simulation results are compared with the state of the art.

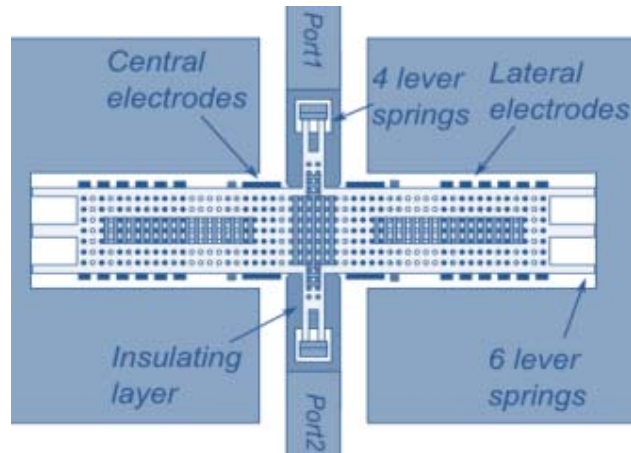
2. Resonator Design

A. MEMS Varicap

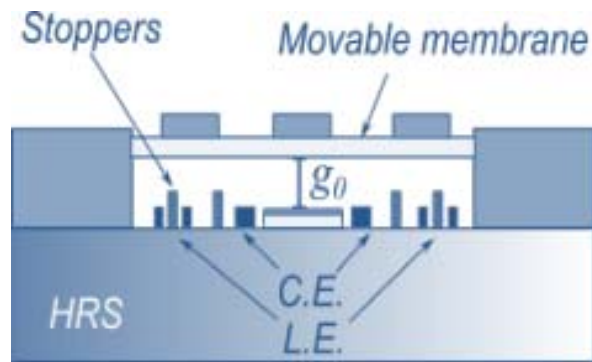
Figure 1 shows the layout and cross-section of the MEMS varactor to be used in the LC tank.

The device consists of a movable membrane placed in shunt configuration with respect to a *coplanar waveguide* (CPW) RF line, on *high resistivity silicon* (HRS) substrate, 625 μm thick. The device is based on a double actuation this purpose, the DC electrodes have been split into two separate electrodes, called L.E. (*lateral electrodes*) and CE (*central electrodes*) as shown in Fig. 1a [9]. When no voltage is applied, the residual gap g_0 is 2.5 μm , (Fig. 1b) and the device shows a measured capacitance of 115 fF. By applying an increasing DC control voltage

from 0 V up to 35 V on the L.E., the capacitance continuously increases up to 185fF, corresponding to a capacitive ratio of about 1.6. For voltages higher than 40



a)



b)

Fig. 1. MEMS Varicap: a) Top view; b) Cross section.

V, the bridge snaps down. However, the complete membrane snap-down above the RF line is avoided thanks to the 4 lever springs in the central part of movable membrane. In this state, the device shows a capacitance of 225 fF. Then, by applying a DC signal from 0 V to 60 V on the C.E., the residual gap is continuously decreased allowing for a further continuous tuning (capacitive ratio (Cr^*) of 2.6 corresponding to a measured capacitance of 600 fF). To sum, the varicap presents two regions of continuous tuning providing an overall capacitive ratio (Cr) of 5.2, Fig. 2.

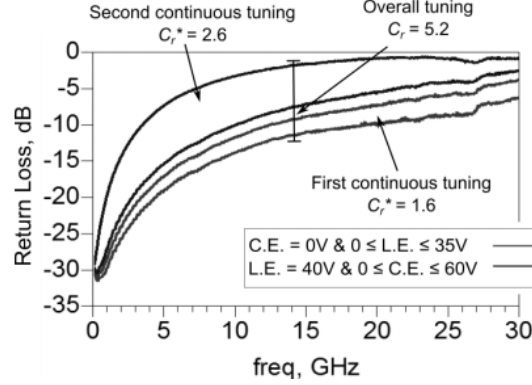


Fig. 2. MEMS Varicap: measured return loss as function of the applied voltage. C_r^* and C_r stand for continuous and non-continuous capacitive ratio.

B. MEMS Spiral Inductor

The proposed spiral inductor is shown in Fig. 3a. It consists of a 5 μm thick gold suspended membrane in circular shape of external diameter D_{ext} of about 440 μm . D_{int} is the internal diameter of the structure. S and w are the spacing among turns and the width of the wire conductor, respectively. The spiral inductor was designed to be manufactured in FBK-irst MEMS process [10], monolithically integrated with the MEMS varicap described above.

Since the suspended structure (Fig. 3b, $g_0 \approx 2.7 \mu\text{m}$) is sensitive to process stresses, a mechanical analysis was performed in ANSYS[®] multiphysics environment in order to simulate the residual stress condition. For the Young modulus (E), the residual stress (σ) and gradient of stress $\sigma(z)$ of the gold membrane, the values of 75 GPa, 60 MPa and 12 MPa were used. Fig. 4a shows the delta displacement ($\Delta - z$) along z axis, just after the release of the structure. The suspended conductor is up-warped of + 0.1 μm and down-warped of - 6 μm , resulting in an unpredictable inductance value, since the coupling capacitance between spirals is abruptly changed. In order to ensure high conductor flatness, mechanical pillars, equally spaced at the distance of about 60 μm , were inserted in the design. Resulting delta displacement ($\Delta - z$) along z axis, just after the release of the structure, is shown in Fig. 4b. 15 $\mu\text{m} \times 15 \mu\text{m}$ square pillars are fabricated below the suspended inductor without changing the manufacturing process.

Afterwards, the device was designed in CPW technology and was simulated in ANSYS[®] HFSS full-wave environment in the 0 – 30 GHz frequency range. HRS substrate, 625 μm thick, was used. The main responsible of the low-Q performance was found to be the thinner metal below suspended conductor, named underpass in Fig. 3b. As consequence, in order to maximize the quality factor (Q)

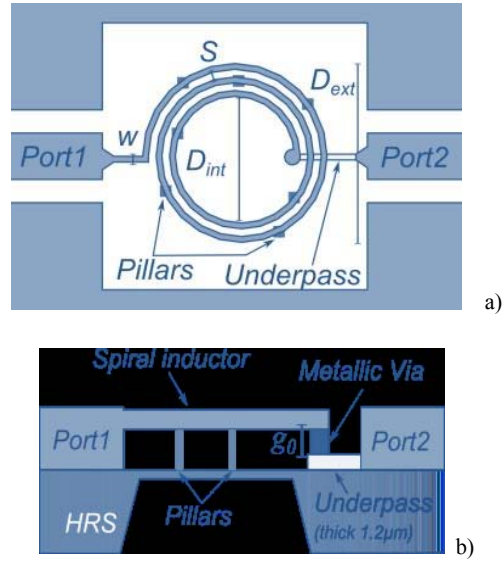


Fig. 3. MEMS spiral inductor: a) Top view; b) Cross section.

and the *self-resonance frequency* (SRF) of the device, two different solutions were implemented: the first one was to increase the thickness of the underpass metal, from the standard value of $0.6\mu\text{m}$ up to $1.2\mu\text{m}$ reducing the conductor loss due to the skin effect. The second one was to partially remove the silicon substrate reducing the substrate loss and the parasitic coupling with the inductor. *Deep reactive-ion etching* (DRIE) will be used to create deep penetration with high aspect ratio in the substrate.

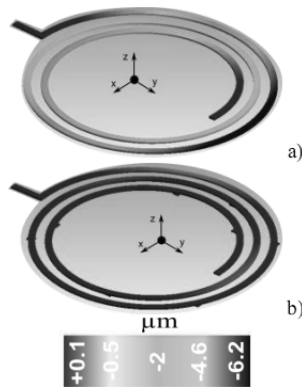
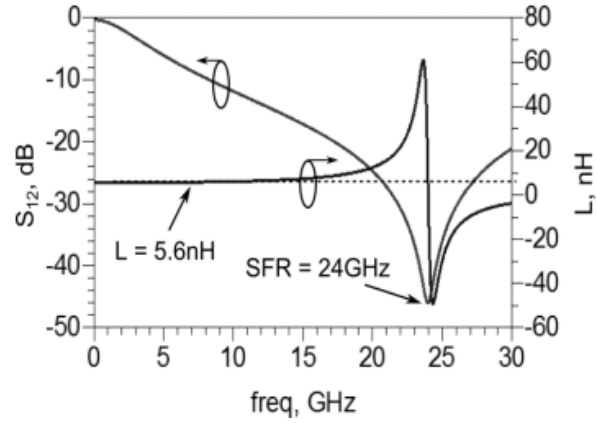


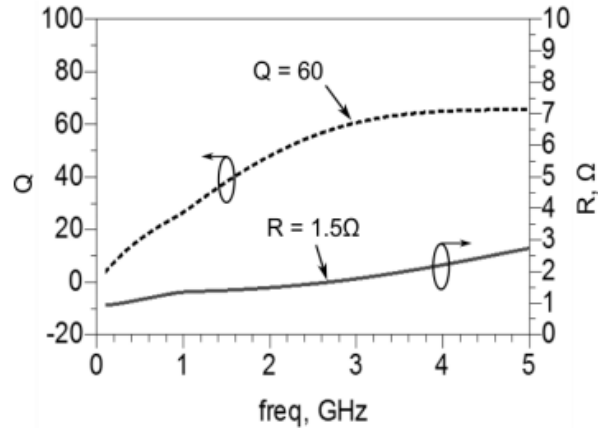
Fig. 4. Delta displacement just after the release of the structure: a) without pillars; b) with pillars.

Simulated S-parameters and inductance (L) are shown in Fig. 5a. In Fig. 5b, the simulated equivalent series resistance (R) and the quality factor (Q) are reported.

Up to 10 GHz, the device exhibits a theoretical inductance of about 5.6 nH. Very high self-resonance frequency (SRF) of about 24 GHz is achieved thanks to the fact that the conductor is suspended. Up to 5 GHz, the resistance is in the range $1\Omega - 2.7\Omega$, resulting in a Q higher than 60 at 3 GHz.



a)



b)

Fig. 5. HFSS simulation results: a) S_{12} , L and b) R, Q for the proposed MEMS spiral inductor.

By using the equivalent π -model circuit, the S-parameters were fitted in ADS circuit environment and equivalent circuitual parameters were extracted. They are

shown in Fig. 6 and result in an inductance value of about 5.8 nH and an equivalent series resistance of 1.6 Ω .

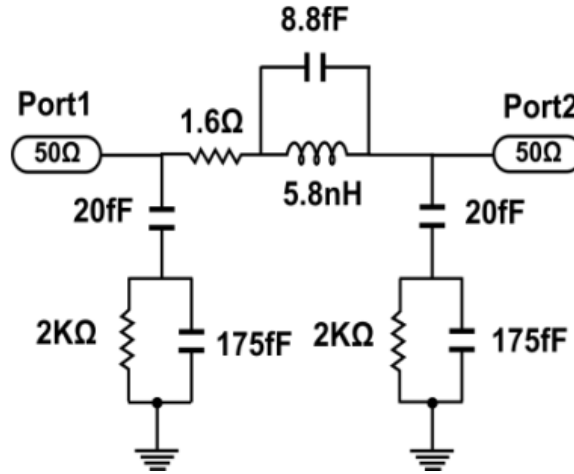


Fig. 6. MEMS spiral inductor: π -model equivalent circuit.

3. Simulation Results of MEMSs Based LC Tank

Finally, the MEMS based series LC resonator was modeled in ANSYS[®] HFSS full wave environment in the 1 – 5 GHz frequency range. Bonding wires were also modeled to account for the interconnection with the VCO active circuitry. The latter will be fabricated in *surface mount technology* (SMT), on a Roger T-Duroid 4350 substrate, 725 μm thick (Fig. 7).

Simulated admittance (real part), as function of the capacitive tuning of the MEMS varicap, is shown in Fig. 8.

The LC resonator shows an overall tuning higher than 60 % in the frequency range 2.15 – 3.85 GHz. Two separate regions of continuous tuning are obtained thanks to the two separate continuous tuning regions of the MEMS varicap. The first one is centered at ~ 3.65 GHz (WiMAX applications) and allows for a continuous tuning up to 9.5% (3.5–3.85 GHz). The second one allows for a continuous tuning between 2.15 – 2.95 GHz, (30%) ensuring to cover all the frequency bands of WLAN and Bluetooth applications.

At last, the quality factor was computed as in [11], and it is greater than 55 in the frequency range 2.15 – 3.85 GHz.

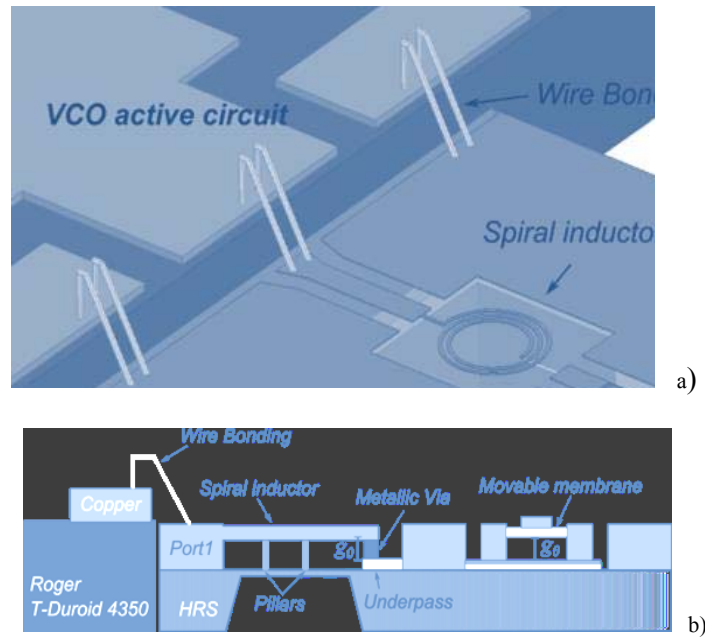


Fig. 7. MEMS based LC tank: a) 3D-model; b) Cross section.

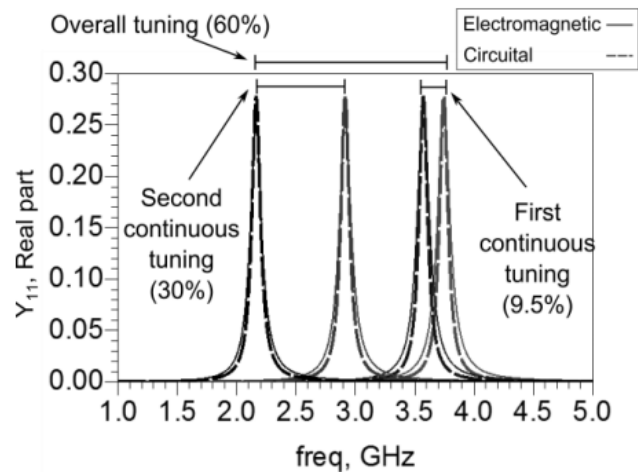


Fig. 8. Simulated full wave (solid line) and circuital (dashed line) admittance (real part) of the MEMS based LC tank.

4. Conclusion

In this paper, the modeling and simulations of a compact multi-band MEMS based LC series resonator has been presented. It is based on a MEMS varicap with an overall capacitive ratio of 5.2 and very high-Q MEMS spiral inductor (~ 60 at 3GHz). The overall size of the device is $2\text{mm} \times 2\text{mm}$. The designed resonator shows an overall tuning range of 60% and two separate regions of continuous tuning (9.5% and 30%). Such a LC tank resonators allows the design of VCOs simultaneously operating in the IEEE 802.11b/g (WLAN), IEEE 802.15x (Bluetooth) and IEEE 802.16d (WiMAX) standards. The comparison with the state of the art about MEMS based resonator has been also presented.

References

- [1] A.B. BASSAT, A.A. KIDWAI, S. RIVEL R. SADHWANI, *Multi -band Multi-standard Local Oscillator Generation for Direct up/down Conversion Transceiver Architectures Supporting WiFi and WiMax Bands in Standard 45nm CMOS Process*, in IEEE Radio Frequency Integrated Circuits Symposium, pp. 149 – 152, 2010.
- [2] Z. XU J. GUO, *Design of Miniature Tri-band Monopole Antenna for WLAN and WiMAX Applications*, in International Conference on Electronic Packaging Technology, 2014.
- [3] M. STEER, *Microwave and RF Design: A Systems Approach*, Scitech Pub Inc, 2009.
- [4] W.B. KUHN and N.M. IBRAHIM, *Analysis of current crowding effects on multiturn spiral inductors*, IEEE Trans. Microwave Theory & Tech., **49**, pp. 31–38, 2000.
- [5] I. BAHL, *Lumped Elements for RF and Microwave Circuits*, Ed. Artech House, 2003.
- [6] D.C. EDELSTEIN, M. SOYUER, H.A. AINSPAN and K.A. JENKINS J.N. BURGHARTZ, *RF circuit design aspects of spiral inductors on silicon*, IEEE J. Solid-State Circuits, **33**, pp. 2028 – 2034, 1998.
- [7] Y.-S. CHOI and J.-B. YOON, *Experimental analysis of the effect of metal thickness on the quality factor in integrated spiral inductors for RF IC's*, IEEE Electron Device Lett., **25**, pp. 76 – 79, 2004.
- [8] G.M. REBEIZ, *RF MEMS : Theory, Design, and Technology*, Wiley, 2003.
- [9] A. CAZZORLA, P. FARINELLI and R. SORRENTINO, *Double-actuation extended tuning range RF MEMS varactor*, in European Microwave Conference, Paris, 6 – 11 september, 2015.
- [10] V. MULLONI, S. COLPO, J. IANNACCI, B. MARGESIN F. GIACOMOZZI and A. FAES, *A Flexible Technology Platform for the Fabrication of RF-MEMS Devices*, in International Semiconductor Conference, Romania, pp. 155 – 158, 2011,
- [11] R. SORRENTINO and G. BIANCHI, *Microwave and RF Engineering*, Wiley, Ed., 2010.
- [12] A.Q. LIU, Q.X ZHANG, A.B. YU, *Tunable MEMS LC resonator with large tuning range*, IEEE Electronics Letters, **21**, pp. 855 – 857, 21 July 2005.
- [13] J.D. MARTINEZ, M. CHATRAS, A. POTHIER, V.E. BORJA and P. BLONDY, R. STEFANINI, *Ku Band High-Q Tunable Surface-Mounted Cavity Resonator Using RF MEMS Varactors*, IEEE microwave and wireless components letters, **21**(5), 2011.
- [14] A. CAZZORLA, P. FARINELLI, R. SORRENTINO, *MEMS based LC tank with extended tuning range for Multi-band applications*, 2015 IEEE 15th Mediterranean Microwave Symposium (MMS), Nov 30 – Dec 2, pp. 1 – 4, 2015.
- [15] www.ansys.com